BIOCHEMISTRY
including biophysical chemistry & molecular biology
Article

Biochemistry **2010,** *49,* 7367–7376 7367
DOI: 10.1021/bi1005305

Crystal Structures and Mutational Analyses of Acyl-CoA Carboxylase β Subunit of *Streptomyces coelicolor*[†,‡]

Ana Arabolaza,[#,∥] Mary Elizabeth Shillito,[#,§] Ting-Wan Lin,[§] Lautaro Diacovich,[∥] Melrose Melgar,[§] Huy Pham,[§] Deborah Amick,[§] Hugo Gramajo,*[,∥] and Shiou-Chuan Tsai*[,§]

[§]*Department of Molecular Biology and Biochemistry, Department of Chemistry, and Department of Pharmaceutical Sciences, University of California, Irvine, California 92697-3900, and* [∥]*Instituto de Biología Molecular y Celular de Rosario (IBR-Consejo Nacional de Investigaciones Científicas y Técnicas) and Departamento de Microbiología, Facultad de Ciencias Bioquímicas y Farmacéuticas, Universidad Nacional de Rosario, Suipacha 531, 2000 Rosario, Argentina* [#]*Contributed equally.*

Received April 8, 2010; Revised Manuscript Received July 19, 2010

ABSTRACT: The first committed step of fatty acid and polyketides biosynthesis, the biotin-dependent carboxylation of an acyl-CoA, is catalyzed by acyl-CoA carboxylases (ACCases) such as acetyl-CoA carboxylase (ACC) and propionyl-CoA carboxylase (PCC). ACC and PCC in *Streptomyces coelicolor* are homologue multisubunit complexes that can carboxylate different short chain acyl-CoAs. While ACC is able to carboxylate acetyl-, propionyl-, or butyryl-CoA with approximately the same specificity, PCC only recognizes propionyl- and butyryl-CoA as substrates. How ACC and PCC have such different specificities toward these substrates is only partially understood. To further understand the molecular basis of how the active site residues can modulate the substrate recognition, we mutated D422, N80, R456, and R457 of PccB, the catalytic beta subunit of PCC. The crystal structures of six PccB mutants and the wild type crystal structure were compared systematically to establish the sequence−structure−function relationship that correlates the observed substrate specificity toward acetyl-, propionyl-, and butyryl-CoA with active site geometry. The experimental data confirmed that D422 is a key determinant of substrate specificity, influencing not only the active site properties but further altering protein stability and causing long-range conformational changes. Mutations of N80, R456, and R457 lead to variations in the quaternary structure of the beta subunit and to a concomitant loss of enzyme activity, indicating the importance of these residues in maintaining the active protein conformation as well as a critical role in substrate binding.

In actinomycetes, the building blocks for fatty acids, complex lipids, and polyketide biosynthesis are provided by acyl-CoA carboxylases (ACCases),[1] enzyme complexes that carboxylate the α-carbon of acetyl-, propionyl-, or butyryl-CoA to produce malonyl-, methylmalonyl-, and ethylmalonyl-CoA, respectively (*1*). ACCases are loosely categorized by their substrate specificity. The ACCase that preferentially accepts acetyl-CoA as a substrate is defined as an acetyl-CoA carboxylase (ACC), while the one that accepts propionyl-CoA as its preferred substrate is defined as a propionyl-CoA carboxylase (PCC) (*2*). Reactions catalyzed by ACCases involve two steps (Scheme 1) (*3*, *4*). In the first reaction, biotin-carboxylase (BC) catalyzes the formation of carboxybiotin (*4*−*8*). The cofactor biotin is attached to the biotin-carboxylase carrier protein (BCCP) like a "swinging arm" (*3*, *9*−*12*). In the second reaction, catalyzed by a carboxyltransferase (CT), the carboxyl group is transferred from carboxybiotin to acetyl- or propionyl-CoA to form malonyl- or methylmalonyl-CoA (*1*, *13*−*16*). In actinomycetes, most ACCases consist of three polypeptides: an α-subunit containing the BC and BCCP domains, a β-subunit corresponding to the CT domain, and an ε-subunit that serves as the adaptor protein between α and β subunits, whose inclusion results in an enhanced enzyme activity (*17*). Two ACCases of *Streptomyces coelicolor*, ACC and PCC, were recently identified and characterized in our laboratories (*17*). ACC and PCC share the same biotinylated subunit, AccA2, while the β and the ε subunits are specific for each complex. Namely, for *S. coelicolor* PCC, the β and ε subunits are designated as PccB and PccE, respectively. Likewise, for *S. coelicolor* ACC the β and ε subunits are designated as AccB and AccE, respectively. In vitro, ACC can carboxylate acetyl-, propionyl-, or butyryl-CoA with approximately the same specificity, while PCC recognizes only propionyl- and butyryl-CoA as

[†]Part of this work was supported by a Fogarty International Research Collaboration Award from the NIH (R03 TW005778 and TW007982). ANPCyT Grant 01-13705 and PIP 6436 CONICET to H.G., by the Pew Foundation and NIH (R01 AI076460 and R03 AI073426 to S.C.T. and by the ASM to A.A. Portions of this research were carried out at the Stanford Synchrotron Radiation Laboratory, a national user facility operated by Stanford University on behalf of the U.S. Department of Energy, Office of Basic Energy Sciences. The SSRL Structural Molecular Biology Program is supported by the Department of Energy, Office of Biological and Environmental Research, and by the National Institutes of Health, National Center for Research Resources, Biomedical Technology Program, and the National Institute of General Medical Sciences. The Advanced Light Source is supported by the Director, Office of Science, Office of Basic Energy Sciences, of the U.S. Department of Energy under Contract No. DE-AC02-05CH11231.

[‡]The atomic coordinates have been deposited in the Protein Data Bank (accession codes 3IBB, 3IB9, 3IAV, and 3MFM).

*To whom correspondence should be addressed. Shiou-Chuan (Sheryl) Tsai: E-mail: sctsai@uci.edu; phone: 949-824-4486; fax: 949-824-8552; Hugo Gramajo: E-mail: gramajo@ibr.gov.ar.

[1]Abbreviations: ACCase, Acyl-CoA carboxylase; ACC, acetyl-CoA carboxylase; PCC, propionyl-CoA carboxylase, PKS, polyketide synthase; AccB, beta subunit of ACC; PccB, beta subunit of PCC; AccE, epsilon subunit of ACC; PccE, epsilon subunit of PCC; AccA2, alpha subunit of ACC or PCC.

Published on Web 07/22/2010

Scheme 1: Stepwise Reactions of ACCase

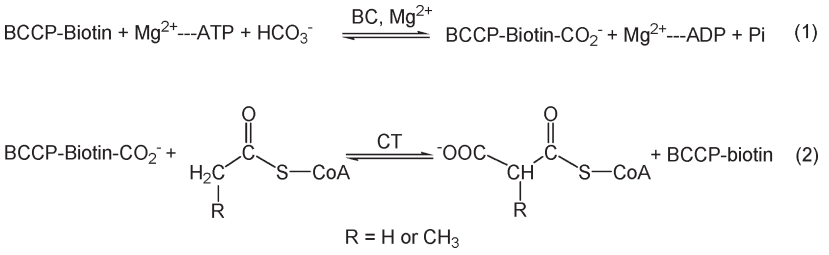

substrates (*17*−*19*). AccB and PccB share 75% of sequence identity. How two highly homologous enzymes such as ACC and PCC could have such different substrate specificities is not well understood.

Besides providing the building blocks for fatty acids biosynthesis, ACCases also catalyze the first committed step of polyketide biosynthesis (*20*). Polyketides consist of a large (> 10 000 compounds) family of structurally diverse natural products (*21*), including antibiotics (such as tetracycline and erythromycin), chemotherapeutics (such as leomycin, doxorubicin, and epothilone), cholesterol lowering drugs (such as lovastatin), antiparasitic agents (such as avermectin), antifungal agents (such as amfotericine B), and immunosuppressants (such as rapamycin and FK506) (*21*). In nature, polyketides are diversified by the controlled variation in chain length, choice of chain-extension units, and optional chain modification. Taking advantage of the built-in flexibility of polyketide synthase (PKS), hundreds of "unnatural" natural products have been produced from engineered PKSs (*21*, *22*). ACC and PCC, in essence, serve as the "gatekeeper" enzyme for polyketide biosynthesis by supplying the specific building blocks, malonyl- or methylmalonyl-CoA, to PKSs (*20*), which are also known to accept a wide variety of synthetic acyl groups as their substrates (*23*−*25*). However, to biosynthesize polyketides with different extender units, it is necessary to have an engineered ACCase with expanded substrate specificity, so that it could accept new acyl-CoA substrates (including non-natural ones) to produce novel extender units. Therefore, an understanding about ACCase substrate specificity at the molecular level can potentially enable the engineering of ACCase with altered substrate/product specificity, so that "unnatural" extender units can further diversify the downstream polyketide biosynthesis.

In our previous studies, using X-ray crystallography, mutagenesis, and enzyme kinetics, we demonstrated that the β subunit is the major determinant of substrate specificity. We further found that residue D422 of PccB (I420 of AccB) in the active site is important for determining substrate specificity. Mutation of D422 to I422 in PccB enables the PCC complex to accept acetyl-CoA as its substrate (*26*). The local environment of Asp422 is hydrophobic in nature. The side chain of this residue is not involved in ion-pair or hydrogen-bonding interaction, while its main chain N and C=O form hydrogen-bond with C=O of G419 and the side chain of Ser426, respectively. This residue is a semi-conserved L or V in ACC, and a nonconserved A or C in most organisms. However, it is unclear how a single amino acid mutation can result in such a drastic change of substrate specificity.

To further evaluate the influence of residue D422 on substrate specificity, herein we present systematic mutations of residue 422 in PccB, the kinetic studies and substrate specificities of these mutants, and the crystal structures of these 422 mutants. These data allow us to compare seven different beta subunit structures, each with a different substrate specificity, and establish the sequence−structure−function relationship of the substrate specificity in PccB that will aid in future protein design for mutant PccB that generates new building blocks for downstream polyketide biosynthesis.

MATERIALS AND METHODS

Chemicals, Strains, and DNA Manipulation. *Escherichia coli* strain DH5α was used for routine subcloning. Transformants were selected on media supplemented with the appropriate antibiotics (100 μg/mL Ap, 20 μg/mL Cm, or 50 μg/mL Km). Strain BL21 λ(DE3) is an *E. coli* B strain lysogenized with λDE3, a prophage that expresses the T7 RNA polymerase from the IPTG-inducible *lac*UV5 promoter (*2*). Rosetta λ(DE3) expresses rare tRNAs to facilitate expression of genes that encode rare *E. coli* codons.

Site-Directed Mutagenesis. Site-directed mutagenesis of the gene coding the β subunit of the PCC complex, PccB, was performed by the Qiagen QuikChange kit. Mutagenesis primers were 30 nucleotides in length with the altered base(s) located at the middle of the sequence. The sequence alterations were conformed by bidirectional sequencing at the UC Davis DNA sequence facility.

Expression and Purification. The mutant *pccB* genes, derived from pTR131 (His6-PccB) (*17*), were inserted into the pET28 vector (Novagen) and were transformed into *E. coli* BL21 λ(DE3). Protein expression was induced by adding 0.1 mM IPTG to cultures grown to A600 = ∼0.8. The wild type and mutant proteins were purified following the same protocol as described by Diacovich et al.(*17*). The biotin carboxylase subunit AccA2 was purified from cultures of BL21 λ(DE3) harboring pTR204 and pCY216, which contains the *E. coli birA* gene to allow high level of biotinylation of AccA2. AccB, AccE, and PccE protein expression and purification were performed as described previously (*17*). Proteins were concentrated by ultrafiltration through a PM-3 membrane (Amicon) or Ultra-15 (ultracel 5K cellulose) (Amicon) and stored at −80 °C.

Coupled Enzyme Assay. The rate of ATP hydrolysis by biotin carboxylase was measured spectrophotometrically (*29*). The production of ADP was coupled to pyruvate kinase and lactate dehydrogenase, and the oxidation of NADH was followed at 340 nm. The assay mixture contained 5 units of pyruvate kinase, 10 units of lactate dehydrogenase, 0.5 mM phosphoenolpyruvate, 0.2 mM NADH, 5 mM $MgCl_2$, 0.3 mg/mL BSA, 100 mM potassium phosphate, pH 7.6, 3 mM ATP, 50 mM $NaHCO_3$, and the appropriate concentrations of acetyl-, propionyl-, or butyryl-CoA. Reactions were initiated by the addition of different enzyme components. The amount of coupling enzymes was sufficient to ensure that the initial velocity varied linearly with the enzyme concentration. Temperature was maintained at 30 °C by a circulating water bath with the capacity to

Table 1: Crystallization Conditions, Crystallographic, and Model Statistics of the PccB Mutants

	D422V	D422L	D422N	D422C	D422A
crystallization	0.1 M Tris pH = 6.5, 2.0 M $(NH_4)SO_4$	0.1 M Tris pH = 6.5, 2.0 M $(NH_4)SO_4$	0.1 M Bis-Tris pH = 6.8, 10% MPD, 0.2 M $(NH_4)OAc$	0.1 M Na citrate pH = 5.6, 0.2 M $(NH_4)SO_4$	0.1 M Bis-Tris pH = 6.2, 20% PEG3350, 0.2 M $(NH_4)SO_4$
			Data Collection		
space group	$P6_3$	$P6_3$	$P2_1$	$P2_1$	$P2_12_12_1$
# monomer in AU	2	2	6	6	6
cell dimension *a*, *b*, *c* (Å)	171.531, 171.531, 75.068,	168.489, 168.489, 80.304,	79.668, 220.961, 136.742,	79.572, 220.786, 136.885,	87.060 183.328 228.706
α, β, γ (°)	90, 90, 120	90, 90, 120	90, 103.08, 90	90, 102.84, 90	90, 90, 90
resolution (Å)	1.75	1.90	2.38	2.95	3.45
mosaicity (deg)	0.82	0.89	0.34	0.73	1.2
no. of observations	1122861	858632	1234057	212259	261634
no. of unique reflections	123433	96803	182019	73274	46012
completeness % (last shell)	97.4 (89.6)	94.1 (98.1)	99.0 (95.8)	86.8 (71.4)	95.3 (96.5)
$I/\sigma(I)$ (last shell)	17.32 (2.8)	23.99 (4.2)	19.35 (3.8)	7.25 (2.1)	11.2 (4.5)
R_{merge} (last shell)	0.145 (0.436)	0.10 (0.517)	0.10 (0.405)	0.148 (0.464)	0.188 (0.497)
redundancy	9.1	8.9	6.8	2.7	5.7
			Refinement		
resolution (Å)	1.75	2.0	2.5	3.2	3.5
no. refinement reflections	113083	66425	149431	63866	43717
no. of protein atoms	7904	7904	23718	23706	23700
no. of waters	323	339	0	0	0
R_{free} %	23.25	25.12	27.56	25.83	26.94
R_{crys} %	21.71	24.87	22.20	19.75	19.03
			Geometry		
rmsd for bonds (Å)	0.0058	0.0057	0.051	0.060	0.059
rmsd for angles (deg°)	1.264	1.287	3.641	4.755	3.950

heat and cool the thermospace of the cell compartment. Initial velocities are obtained from initial slopes of the recorder traces. Under the assay conditions described, the reaction was linear for at least 3 min, and the initial rate of reaction was proportional to the enzyme concentration. One unit of enzyme activity catalyzes the formation of 1 μmol of the respective carboxylated CoA derivative or ADP/min under the assay conditions described. Specific activity is expressed as units/mg of AccA2. Essentially identical activities are measured by the $^{14}CO_2$ fixation method (*17*) and by this spectrophotometric method. To obtain the Michaelis−Menten constants K_m and k_{cat}, data were fitted directly to the Michaelis−Menten equation, rate = [enzyme]*[substrate]*k_{cat}/(K_m + [substrate]), using the program Kaleidagraph (Synergy).

Oligomeric State of the β Subunits. Molecular mass was estimated by size exclusion chromatography using a ΔKTA basic high-performance liquid chromatography (Amersham). Samples containing around 200 μg of PccB or the PccB mutant proteins were loaded onto a Superdex S200 column (Amersham) equilibrated and eluted in 50 mM potassium phosphate, pH 7.6, 150 mM NaCl, and 0.5 mM DTT. The column was calibrated with the following molecular mass standards: blue dextran, 2 000 000; thyroglobulin, 669 000; apoferritin, 443 000; β-amylase, 200 000; alcohol dehydrogenase, 150 000; bovine serum albumin, 66 000; and lysozyme, 14 300.

Crystallization of PccB. Crystals of the D422 mutant PccB were grown in sitting drops at room temperature by vapor diffusion. The protein buffer was 10 mM HEPES, pH 7.0, 2 mM DTT. Drops were generated by mixing 2 μL of the purified protein solution with 2 μL of well buffer above well solution of 500 μL. The crystallization conditions for each crystal form are listed in Table 1. When the mutant crystals were grown in similar crystallization conditions, the overall conformation may be similar, and the different substrate specificity may reflect a change of pocket shape (detailed in Discussion).

Data Collection. X-ray diffraction data of PccB were collected at Advanced Light Source (ALS) and Stanford Synchrotron Radiation Laboratory (SSRL) to 2.6−3.4 Å (Table 1). Crystals were frozen according to different crystal forms (Table 1), mainly in 30% glycerol + 70% well solution. The crystal space groups and cell dimensions are listed in Table 1. Diffraction intensities were integrated, reduced using the program DENZO, and scaled using SCALEPACK (*27*). A summary of the crystallographic data is shown in Table 1.

Molecular Replacement and Refinement. Initial phases were determined by molecular replacement, using the crystal structure of wild type PccB as the search model (PDB Code 1XNY). Cross-rotational search followed by translational search was performed utilizing the program CNS (*28*). After the structure was rebuilt using Quanta, further refinement was performed using CNS (*28*). The noncrystallographically related monomers were treated as rigid bodies and were refined using CNS to give an initial R_{crys} of 30%. A preliminary round of refinement using torsion angle simulated annealing, followed by energy minimization, positional and individual B-factor refinement reduced R_{crys} to 27%. Subsequent rounds of model building and refinement were carried out using the maximum likelihood based approach implemented within CNS using all data to the highest resolution. Strict noncrystallographic symmetry restraints were applied for the first round of refinement and then released for subsequent

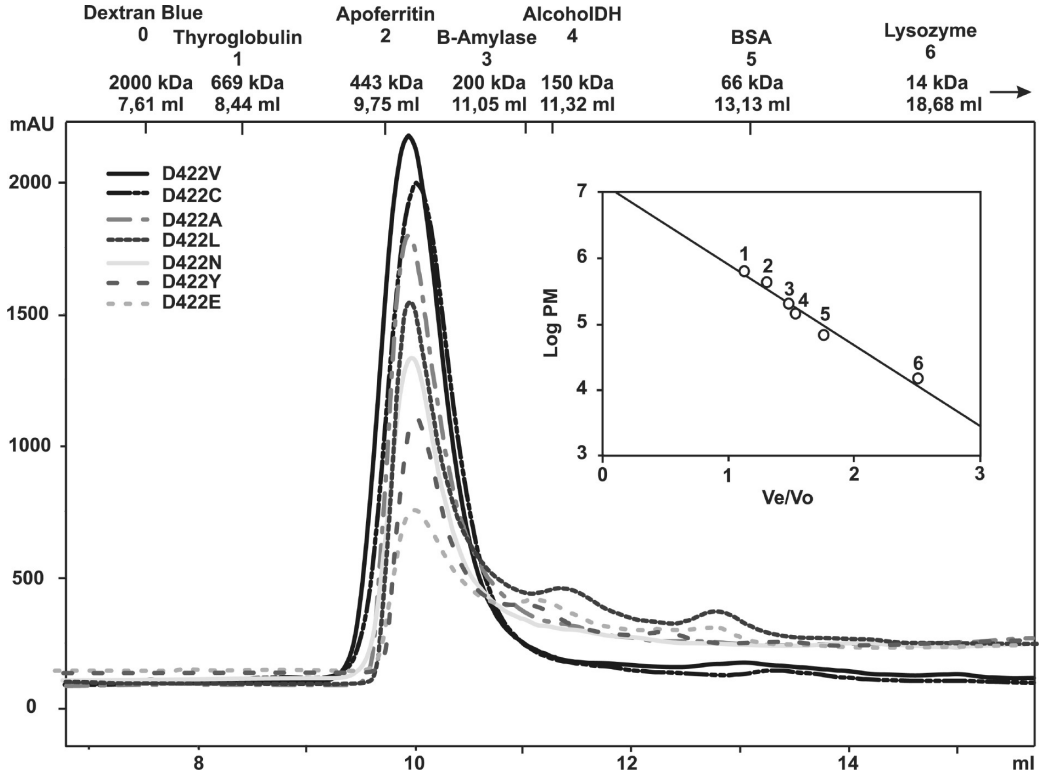

FIGURE 1: Determination of the oligomeric state of PccB mutants. Each D422 mutant was analyzed by size exclusion chromatography (Superdex 200). The protein profiles (A215 in milli-absorbance units [mAU]) and molecular masses of protein standards used for calibration are detailed in the chromatograms.

model building of each monomer. Refinement was continued to an R_{crys} of $<25\%$ ($R_{free} < 27\%$). Table 1 lists the statistics for refinement and components of the final model. After the R_{free} decreased below 0.25, water molecules were added using CNS, followed by visual inspection of the water molecules and final refinement of the B factor.

RESULTS AND DISCUSSION

Mutagenesis, Expression, and Purification of the D422 Mutants. To further analyze the role of Asp 422 in determining the substrate specificity of PccB, we systematically mutated this residue to 19 other amino acids. The resulting single mutants and the wild type enzyme were overexpressed as His_6-fusion proteins in *E. coli* BL21 λ(DE3) to allow for rapid purification on a Ni^{2+} affinity column. The levels of expression were similar for the wild type enzyme and for most of the D422 mutants with a final yield of about 75−100 mg of soluble protein per liter of cell culture when D422 is mutated to Gln, Ala, Asn, Phe, Tyr, Cys, Glu, Ile, Leu, or Val, while most other mutations resulted in inclusion bodies. The analysis of all the D422 mutants by anion-exchange (HiTrap Q) and size exclusion chromatography (Superdex 200) showed that all them, with the exception of D422F and D422Q, presented elution profiles very similar to that of the wild type enzyme PccB (Figure 1). In the cases of D422F and D422Q, the size exclusion chromatography results (performed with protein purified from the soluble fraction) indicated that neither of them could assemble in the active hexameric conformation as the wild type enzyme; instead they showed a mixture of dimer, trimer, and aggregates, indicating protein instability due to the mutation introduced.

Because we previously demonstrated that a successful formation of a $\beta-\varepsilon$ subcomplex was essential in order to obtain a fully active PCC enzyme (*17*), we further analyzed the ability of the PccB mutants to form a stable $\beta-\varepsilon$ interaction. Native PAGE analysis revealed that all the PccB mutants, with the exception of D422F and D422Q, can form a stable $\beta-\varepsilon$ complex, similarly to the wild type PccB-PccE (*17*) (data not shown). These results suggest that purified D422 mutants, with the exception of D422F and D422Q, did not undergo major structural changes that could alter the protein interface between the β and ε subunits.

Kinetic Characterization of the PccB Mutants. The kinetic constants for acyl-CoAs substrate utilization by the wild type and D422 mutants are summarized in Table 2. On the basis of the kinetic parameters, four types of behavior are observed (*1*): D422A, D422C, and D422V behave similarly to the wild type PccB, accepting both butyryl- and propionyl-CoA as their substrates. Interestingly, the substitution of Asp D422 by Ala or Cys resulted in a clear shift in substrate preference from propionyl- to butyryl-CoA (Table 2). In the wild type PccB, the V_{max}/K_m of propionyl-CoA is 2.1 fold higher than that of butyryl-CoA; in comparison, in D422A and D422C, the V_{max}/K_m of butyryl-CoA is 2.3- and 1.2-fold higher than that of propionyl-CoA, respectively. The D422V mutant, in comparison, did not show changes in substrate specificity, compared with PccB (*2*). As reported previously, D422I PccB mutant showed a clear change in substrate specificity since besides propionyl- and butyryl-CoA it was also able to accept acetyl-CoA as a substrate, similarly to AccB (*26*). Because PccB does not normally accept acetyl-CoA as a substrate, the Asp to Ile mutation in PccB results in an expansion of its substrate tolerance. Further, the V_{max}/K_m ratio between acetyl-, propionyl-, and butyryl-CoA is similar between wild type AccB and the D422I PccB mutant (Table 2) (*3*). D422L and D422N mutants have narrowed down their substrate specificity, accepting only propionyl-CoA as their substrate (*4*).

Table 2: Kinetic Parameters for the Wild Type AccB, PccB, and the PccB D422 Mutants[a]

	acetyl-CoA			propionyl-CoA			butyryl-CoA		
enzyme[a]	K_m (μM)	V_{max} (mU/min mg prot.)	V_{max}/K_m[b]	K_m (μM)	V_{max} (mU/min mg prot.)	V_{max}/K_m	K_m (μM)	V_{max} (mU/min mg prot.)	V_{max}/K_m
				Accepts propionyl- and butyryl-CoA					
PccB WT	ND	ND		76 ± 5	1063 ± 21	13.9	104 ± 27	690 ± 65	6.6
D422A	ND[c]	ND		262 ± 9	451 ± 52	1.7	59 ± 38	230 ± 34	3.9
D422C	ND	ND		56 ± 12	335 ± 16	5.9	36 ± 6	262 ± 10	7.1
D422V	ND	ND		77 ± 22	415 ± 22	5.3	383 ± 44	452 ± 10	1.1
				Accepts acetyl-, propionyl-, and butyryl-CoA					
AccB	100 ± 22	432 ± 27	4.3	92 ± 10	620 ± 21	6.7	99 ± 12	439 ± 17	4.4
D422I	335 ± 46	470 ± 23	1.4	315 ± 52	1006 ± 62	3.2	317 ± 30	832 ± 27	2.6
				Accepts only propionyl-CoA					
D422L	ND	ND		159 ± 28	418 ± 20	2.7	ND	ND	
D422N	ND	ND		123 ± 38	498 ± 41	4.0	ND	ND	

[a]Measured by the PK coupled assay, with AccA2-AccB-AccE or AccA2-PccB-PccE. [b]The specificity constant is calculated as V_{max}/K_m, with the unit mU/min•μM•mg protein. [c]ND, not detected.

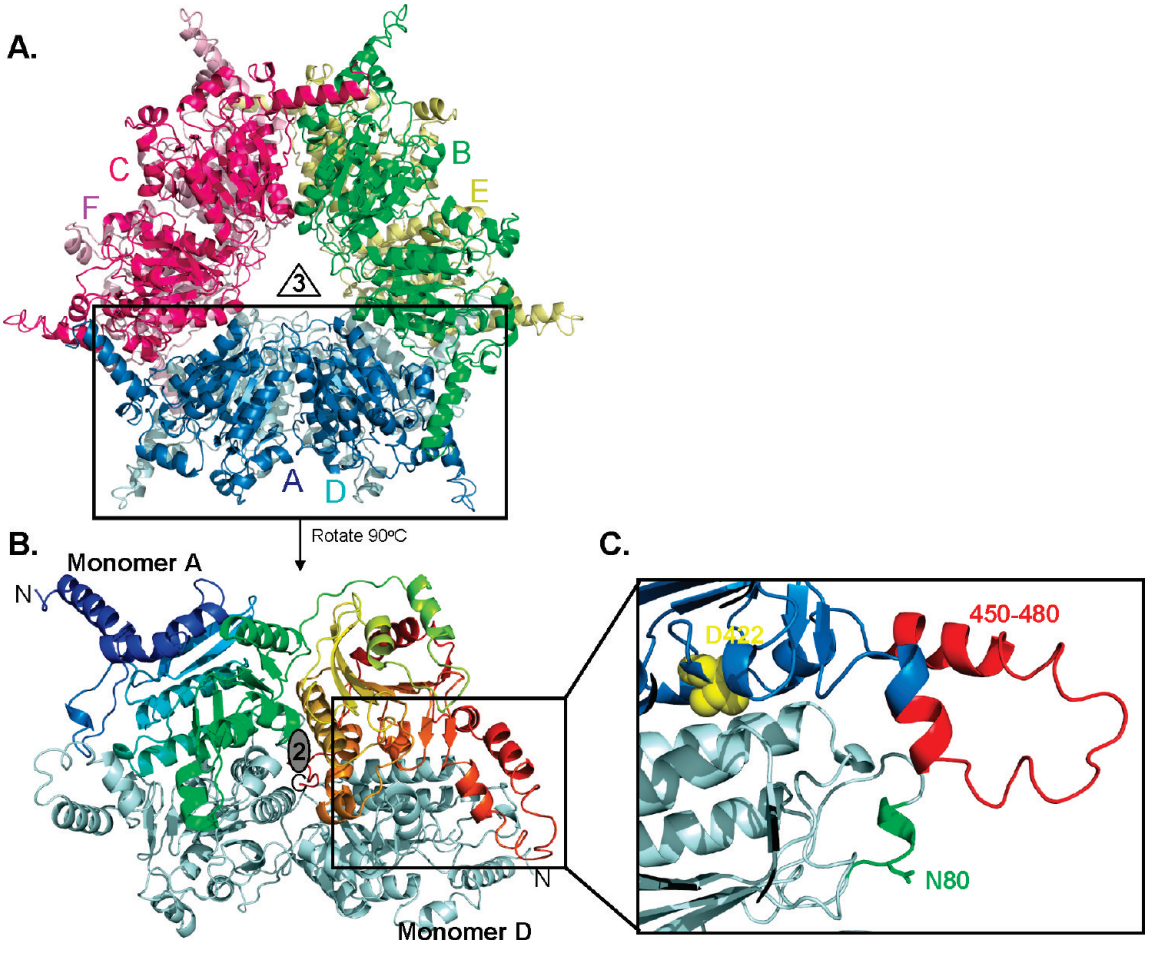

FIGURE 2: (A) The overall structures of all PccB mutants are highly similar as a hexamer, with each monomer in a different color. (B) The PccB active site lies in between two monomers (in color and gray, respectively). (C) Zoom to the acyl-CoA binding pocket, showing the position of residue D422 at the "end" of the active site and the conformation of loops that contain N80 and R456 and R457, which define part of the acyl-CoA pocket entrance.

The mutation of Asp422 to Tyr, Phe, Gln, and Glu completely deactivates the enzyme.

Wild type PccB, as well as all the active PccB mutants, form a highly homogeneous hexamer, as detected by size exclusion chromatography. Interestingly, although D422Y and D422E were also detected as hexamers (Figure 1) and produced stable $\beta-\varepsilon$ interaction (data not shown), they completely lost the enzyme activity, possibly due to subtle changes of the active site

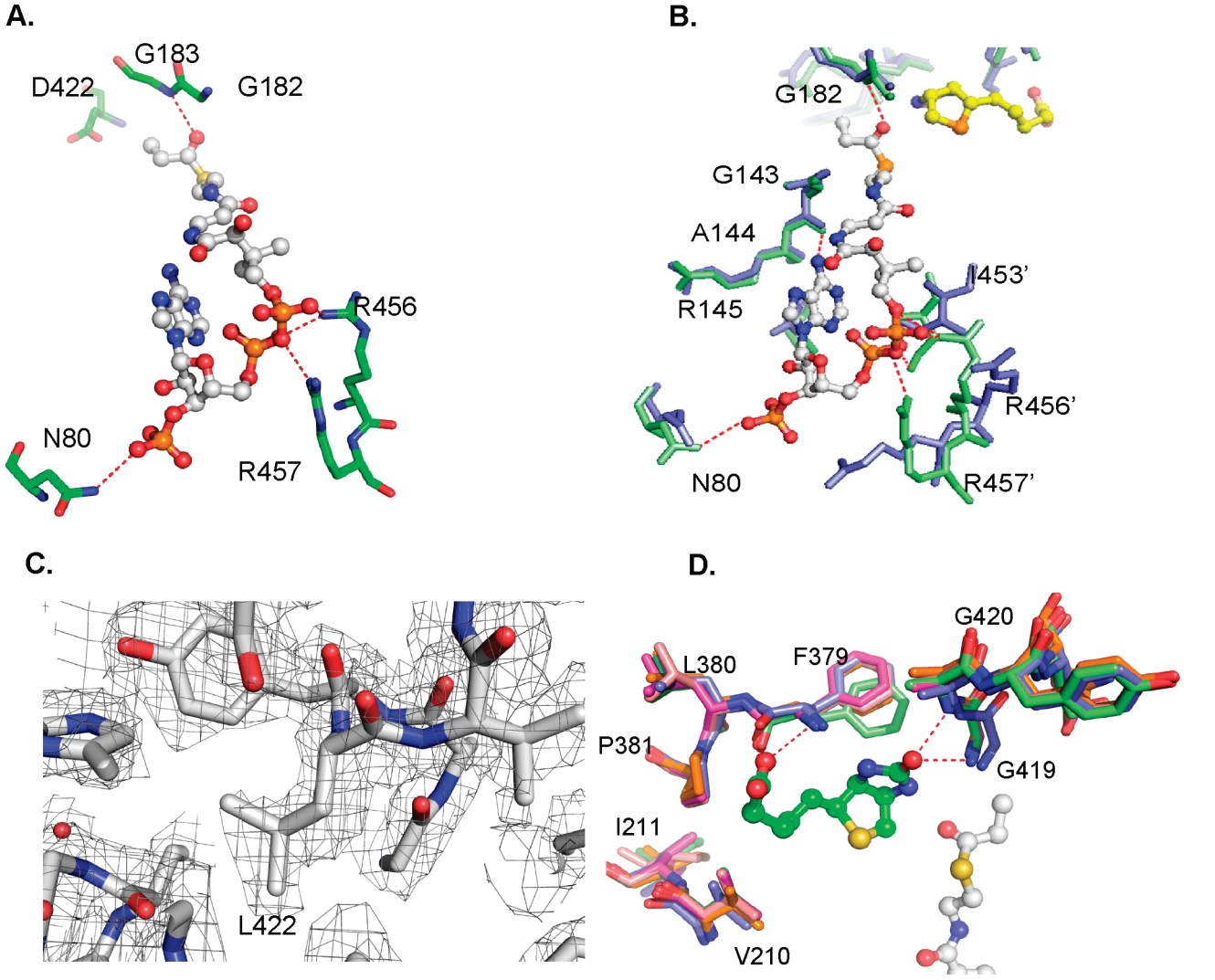

FIGURE 3: (A) Interactions of the CoA phosphate groups with residues N80, R456, and R457 via hydrogen bonds in wild type PccB. (B) Enlarged view, structural overlap between the wild type (green) and D422N mutant (blue), showing the conformational changes near the 55−70 and 450−460 loops. (C) The $F_o - F_c$ simulated annealing electron density map near residue 422 for D422L, contoured at 2.5σ. (D) Structural overlap of the biotin binding pockets of all the PccB mutant shows that there is no significant conformational change in the biotin binding pocket. In the enlarged panels (B), residue 422 is out of sight but is located above the viewpoint.

conformation that inactivates the enzyme while retaining the hexameric stoichiometry.

The above results support our earlier hypothesis that residue 422 of PccB is a key determinant of substrate specificity, and show that most D422 mutants do not significantly change the oligomeric state of the protein or the $\beta-\varepsilon$ interaction upon the single mutation.

Crystal Structures of D422 Mutants Show Conformational Changes in Two Loop Regions. To identify possible conformational changes that result from the D422 mutations, and to synthesize a structure−function correlation between the mutation and observed substrate specificity in these mutants, we solved the crystal structures of D422A, D422C, D422V, D422L, and D422N. The inactive D422Y and D422E mutants cannot be crystallized due to protein instability at high concentration. We then compare these five new mutant structures with the reported wild type PccB, D422I PccB, and I420D AccB structures (*26*). The new series of mutant structures allowed a critical analysis of protein conformational changes caused by mutations.

Consistent with the size exclusion chromatography results, the mutant crystal structures are highly similar to the structures of wild type and D422I PccB, with 0.4−0.7 Å rmsd. The different crystallization conditions (Table 1) may reflect different protein conformations or crystal packing. All mutant structures are hexamers as two stacks of trimers, and each monomer contained two repeats of the crotonase fold (Figure 2A,B). The largest structural deviations occurred in two loop regions between residues 55−70 and 450−460, where the single mutation at residue 422 results in a long-range conformational change at the entrance of the acyl-CoA binding pocket (Figures 2C, 3A,B, S1A), near loop residues 55−70 and 450−460, whose C-α trace deviates 3−5 Å from those of the wild type PccB. The conformational changes in the 55−70 and 450−460 loops result in a large displacement of the side-chains of key residues that interact with the coenzyme A phosphate moiety, such as the side-chains of N80, R456, and R457 (Figure 3A). These structural deviations in the acyl-CoA pocket entrance could decrease the interactions between the protein and CoA phosphates.

The Molecular Basis of Observed Substrate Specificity: Pocket Size versus Phosphate Binding. The kinetic data combined with the structural comparisons carried out between the wild type PccB and the six D422 mutant structures (D422L,

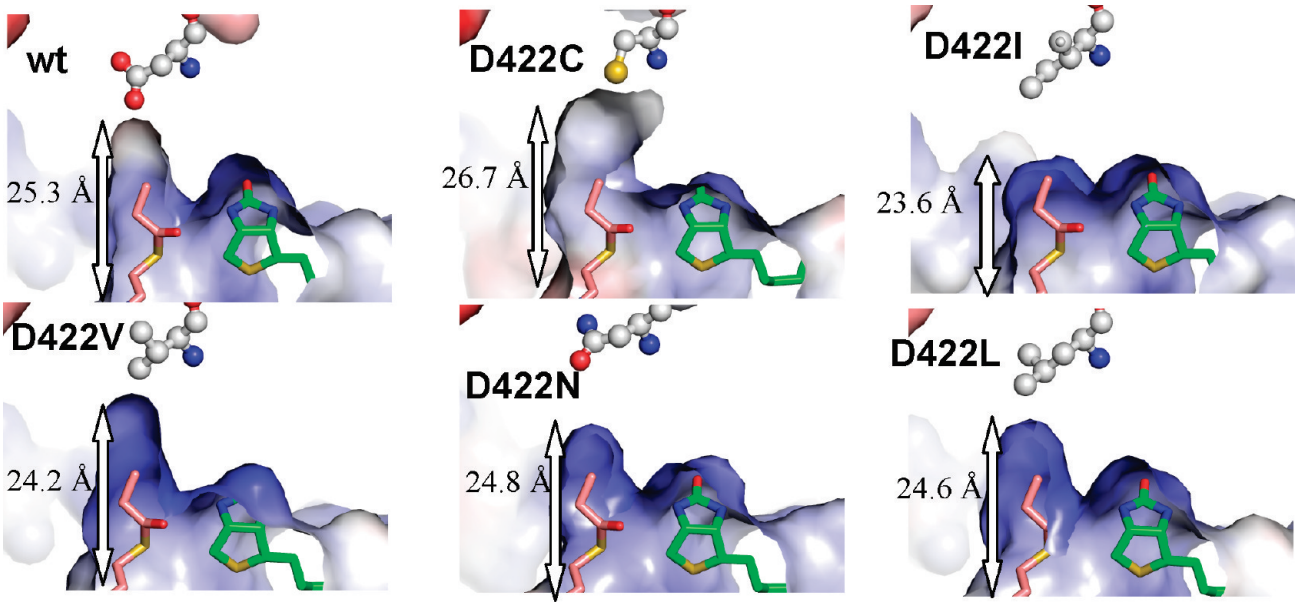

FIGURE 4: A comparison of acyl-CoA binding pocket between wild type and PccB mutants. The molecular surface is colored from red to blue according to electronegative to electropositive surface potential. The labeled length measures the distance from the entrance (the N80 side chain) to the bottom (residue 422 side chain) of the acyl-CoA binding pocket. As a molecular ruler, propionyl-CoA and biotin were docked into the apo mutant structures based on the cocrystal structure of the wild type substrate−biotin complex.

D422N, D422A, D422C, D422V, and D422I) offer the following structural explanation in relation to the observed differences in substrate specificity (Table 2):

(*1*). *Biotin Binding*. In all seven crystal structures, the biotin binding pocket can be overlapped almost perfectly (Figure 3D). Therefore, the observed changes of substrate specificity in D422 mutant is not related with conformational changes in the biotin binding pocket but rather is influenced mainly by conformational changes in the acyl-CoA binding pocket.

(*2*). *Propionyl-CoA Binding*. All the mutants that retain the native PccB conformation (as observed by the crystal structures) accept propionyl-CoA as their substrate. In PccB, the side chain of N80 is the key residue that interacts with the CoA 3′-phosphate, while the side chains of R456 and R457 interact with the CoA pyrophosphate (Figure 3A). N80 and R456-R457 are located in the two loop regions with major conformational changes between the wild type PccB and the D422 mutant structures (Figures 2C, 3B, S1). The conformational changes in the mutant structures could weaken the enzyme-CoA interactions and substrate binding, but not to the extent of completely losing its capacity of binding propionyl-CoA, the natural substrate that the PccB pocket is built to accommodate.

(*3*). *Butyryl-CoA Binding*. The wild type PccB, and D422A, D422C, and D422V mutants accept both propionyl- and butyryl-CoA as their substrates (Table 2). Significantly, D422A and D422C have a higher V_{max}/K_m for butyryl-CoA than for propionyl-CoA. A close examination of the acyl-CoA binding pocket of these PccB mutant structures revealed that they have a larger pocket than D422L and D422N (two mutants that do not accept butyryl-CoA as their substrate). The enlargement of the pocket is evident by the increasing distance from the entrance (N80) to the bottom (residue 422) of the acyl-CoA binding pocket (Figures 4 and S1). Presumably, a larger acyl binding pocket is necessary to accommodate the larger butyryl group. The increase of pocket dimension also helps to explain the increasing affinity for butyryl-CoA in D422A and D422C, since both structures show a longer acyl binding pocket than the wild type PccB. Note that the D422A and D422C mutations also result in a more electropositive pocket due to the replacement of an Asp to the neutral Ala and Cys (Figures 4 and S1). Therefore, although the interactions of D422A, D422C, and D422V with the CoA 3′-phosphate and pyrophosphate are weakened by the loop conformational change around N80 and R456−457 (although not as severe as in the D422N and D422L mutants), the weakening of the phosphate−enzyme interaction may be compensated by the strengthening of van der Waals interactions of the butyryl group (versus the propionyl group) near residue 422 (Figures 3 and 4).

(*4*). *Acetyl-CoA Binding*. D422I is the only PccB mutant that accepts acetyl-CoA as a substrate (*26*). An examination of its acyl-CoA binding pocket shows that D422I has the shortest length from entrance to the bottom of the pocket among the seven solved structures (Figure 4). However, it also retains a strong protein-CoA phosphate interaction at positions N80, R456, and R457 (*26*). Therefore, the ability of an ACCase to bind acetyl-CoA may require both strong protein-CoA phosphate interactions and a smaller acyl-CoA binding pocket in order to provide enough van der Waals interactions between the acetyl group and the amino acids located within the acyl-CoA binding pocket near residue 422. Interestingly, D422I can also bind butyryl-CoA (Table 2, (*26*)). Note that D422I presents very little conformational changes compared to the wild type enzyme, with both the N80 and R456-R457 in place to interact with the CoA phosphate. This observation leads to the hypothesis that butyryl-CoA may still bind to D422I via the strong protein-CoA phosphate interaction, while the acyl-CoA binding pocket undergoes minor conformational changes as an induced fit in solution, but not in the crystal structure, to accommodate the butyryl group.

On the basis of the above structural analysis, the condition for the enzyme to accept butyryl-CoA could be either a longer acyl group binding pocket (such as the wild type PccB, D422A, D422C, and D422V) or a stronger protein-CoA phosphate interaction (such as D422I). However, for the enzyme to accept acetyl-CoA as its substrate, both CoA phosphate-enzyme interactions

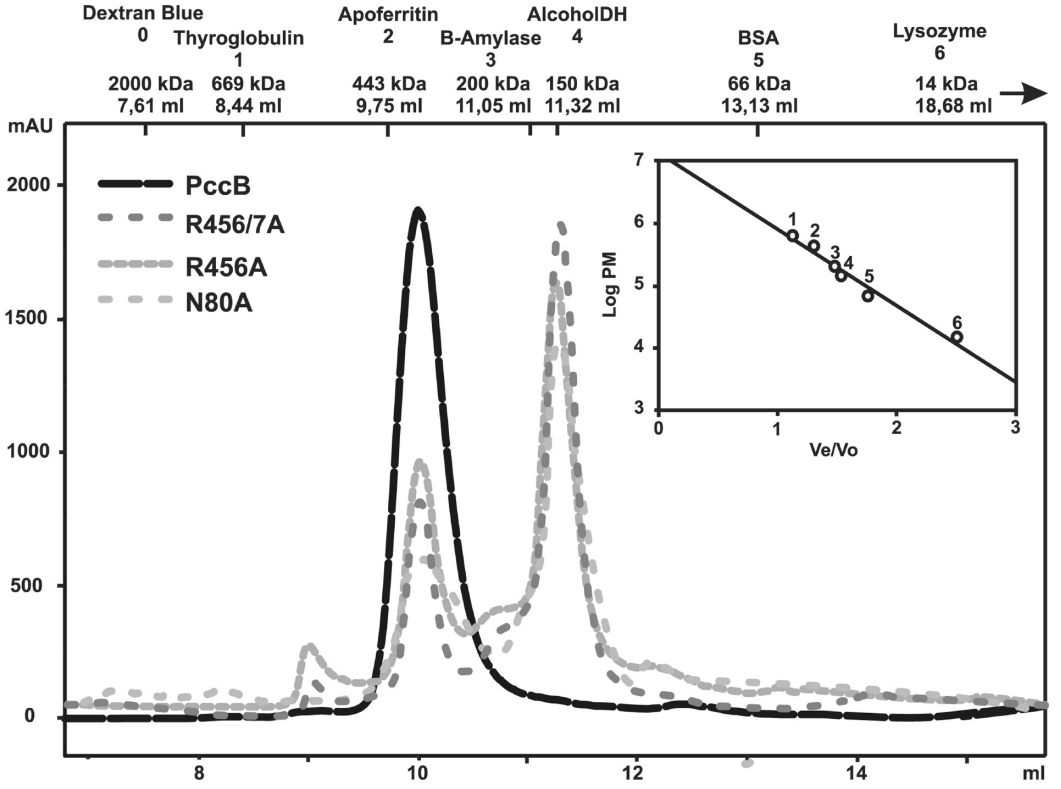

FIGURE 5: Size exclusion chromatography of N80A, R456A, and R456A-R457A mutants. The protein profiles (A215 in milli-absorbance units [mAU]) and molecular masses of protein standards used for calibration are detailed in the chromatogram.

(at N80 and R456-R457) and a small acyl-CoA binding pocket are required. The active site conformations of the wild type and the D422A, D422C, and D422V enzymes satisfy the requirement for propionyl- and butyryl-CoA binding, resulting in their reactivity with only propionyl- and butyryl-CoA. The longer acyl-CoA binding pocket also results in a strong preference for butyryl-CoA in D422A and D422C. In comparison, the active site conformation of D422I satisfies the binding requirement of all three acyl-CoAs, resulting in the activity to bind acetyl-, propionyl-, and butyryl-CoA. The above analyses could also explain the inability of the D422N and D422L mutants to carboxylate butyryl-CoA. Interestingly, the surface charge potential is different for D422V and D422L (Figure 4). The mutations may likely cause a long-range conformational change that affects the acyl-CoA binding pocket, which may result in the change of the charge potential in this binding pocket. Therefore, in these two mutants, the attenuation of the CoA phosphate−enzyme interaction, due to the large conformational changes of the R456−457 and N80 loop regions, combined with the relatively shorter acyl-CoA binding pockets, might result in their inability to bind butyryl-CoA. We conclude that mutations of residue 422 affect the ACCase substrate specificity by altering the size and electronic property of the acyl-CoA binding pocket, but also producing long-distant conformational changes of two loops important for protein-CoA phosphate interactions.

Mutations of N80, Arg456, and Arg457 Support the Importance of Protein-CoA Phosphate Binding. The wild type PccB-acyl-CoA cocrystal structure reveals that the CoA-phosphates form hydrogen bonds with the side chains of N80, R456, and R457 (Figure 3A). To evaluate the importance of N80, R456, and R457 on substrate binding, we generated, expressed, and purified N80A, R456A, and R456A/R457A mutants. Size exclusion chromatography showed that N80A, R456A, and R456/457A exist as a mixture of dimer and hexamer in a 2.0:1.0, 2.2:1.0, and 2.9:1.0 ratio, respectively, while the wild type protein run dominantly as a hexamer (Figure 5). Furthermore, the fraction containing the hexamer of the purified N80A, R456A, and R456/457A did not show enzyme activity in the presence of acetyl-, propionyl-, or butyryl-CoA (data not shown). This observation suggests that residues N80, R456, and R457 may serve the dual role as a provider for the critical protein-CoA phosphate interactions at the entrance of the active site, as well as active participants in stabilizing the hexameric architecture of PccB.

K_m Comparison Shows D422I May Undergo Pocket Conformational Change. The K_m of D422I is unique among the PccB mutants (Table 2). For propionyl-CoA, the K_m is ~100 μM for most mutants except for D422A and D422I ($K_m \sim 300$ μM). The alanine mutation in D422A shifts its substrate affinity toward butyryl-CoA ($K_m \sim 50$ μM), indicating that D422A is capable of binding an acyl-CoA with a similar K_m as that of the wild type enzyme. Therefore, the larger K_m for propionyl-CoA in D422A is likely due to weakened protein-CoA phosphate interactions that can only be compensated in the presence of a butyryl group (with additional van der Waals interaction near residue 422). In comparison, in D422I, the K_m values for acetyl-, propionyl-, and butyryl-CoA are consistently larger (~300 μM) than the K_m of all the other mutants, which contradicts with the observation that D422I has strong protein-CoA phosphate interactions. Because of the small pocket size of D422I, this mutant may need to undergo substantial pocket conformational change before it can accept propionyl- and butyryl-CoA as its substrates. Therefore, extra conformational change step(s) before the formation of the enzyme−substrate complex may become partially rate limiting, resulting in the observed larger K_m values.

Biological Significance. Acetyl-CoA carboxylase (ACC) has been recognized as one of the most important metabolic

checkpoint in living organisms (*29*−*31*), as well as attractive targets for drug discovery against cancer, obesity, diabetes, and microbial infections (*32*). Moreover, the inhibitors of plant ACC, such as the aryloxyphenoxypropionates (FOPs and APPs) and cyclohenediones (DIMs or CHDs), have been commercially used as herbicides for the last 20 years (*33*). In spite of the widely appreciated importance of ACC (*34*−*37*), there is still a critical gap in the knowledge base about how ACC and propionyl-CoA (PCC) recognize different acyl-CoAs as their substrates. Such a knowledge gap, in particular the lack of a sequence-structure−function relationship to correlate ligand-enzyme binding, has hampered the development of ACC-specific therapeutics.

Actinomycetes ACCases have started to emerge as an important group of enzymes with a wide array of essential physiological roles in accordance with their substrate specificity. For instance, ACCases with ACC or PCC roles have been characterized biochemically and structurally in *Streptomyces* and *Mycobacterium* (*17*, *26*, *38*, *39*), and these studies have contributed to the understanding of the ACCase substrate specificity. Moreover, several other CT-encoding genes can be identified in the genome of disease-causing pathogens, whose enzyme activity and physiological role still wait to be elucidated. For example, AccD4 of *Mycobacterium tuberculosis* is presumably the CT of an ACCase complex that carboxylates a C_{26} acyl-CoA; however, its biochemical and structural characterization has not yet been accomplished (*40*). Undoubtedly, the structural characterization of these enzymes will bring not only the opportunity to identify new inhibitors that could develop new antibacterial drugs, but it will also provide important information about the molecular rules that control the ACCase substrate specificity.

Although our previous single mutation work implies the importance of residue 422 on substrate specificity (*26*), we did not conduct systematic mutations of this residue previously. In this work, we have presented a detailed analysis of six D422 mutant PccB structures which, when compared with the wild type PccB crystal structure, have shed light on the effects of D422 mutations. Alterations of this residue, located at the bottom of the acyl-CoA binding pocket, not only change the size, shape, and electronic property of the acyl-CoA binding pocket, but interestingly also result in long-range conformational changes that affect protein-CoA phosphate binding. Phosphate binding has shown to be critical for CoA-binding enzymes. For example, the *Saccharomyces cerevisiae* myristoyl-CoA:protein *N*-myristoyltransferase (Nmt1p), which catalyzes the transfer of myristic acid (C14:0) from myristoyl-CoA to the N-terminus of cellular proteins, cannot react with substrates whose CoA 3′-phosphate is removed (*41*). Similarly, in a detailed study on the effect of CoA 3′-phosphate on human liver medium-chain acyl-CoA dehydrogenase (MCAD), the mutation of an Asn on the MCAD surface that is essential for enzyme−phosphate interaction also significantly affects substrate binding (*42*), illustrating the importance of the enzyme−phosphate interactions. The same study also revealed that the phosphate−enzyme interaction is an energetically dominant factor (in terms of binding enthalpy) between the enzyme and a given acyl-CoA substrate (*42*). Similar results were reported on an isothermal microcalorimetry study on acyl-CoA binding to bovine acyl-CoA binding protein (ACBP), showing that its binding affinity of acyl-CoA is strongly dependent on the length of the acyl chain, and that the 3′-phosphate of the ribose accounts for almost half of the binding energy (*43*). Here, we showed that a single mutation can profoundly affect the substrate specificity via both short-range and long-range effects, and that phosphate−enzyme interaction in the ACCase is, similar to other acyl-CoA binding enzymes such as MCAD, ACBP, and Mnt1p, a key factor that contributes to substrate recognition. In the future, the structure−function−sequence relationship gleaned from this work will allow us to design new PccB mutants, on top of the 422 residue mutation, that accept unnatural acyl-CoAs as its substrates, which may serve as new building blocks for downstream biosynthesis of new "unnatural" natural products such as polyketides (*21*).

SUPPORTING INFORMATION AVAILABLE

Structural comparison of D422A with wild type PccB. This material is available free of charge via the Internet at http://pubs.acs.org.

REFERENCES

1. Lynen, F. (1979) New experiments of biotin enzymes. *CRC Crit. Rev. Biochem. 7*, 103–119.
2. Jitrapakdee, S., and Wallace, J. C. (1999) Structure, function and regulation of pyruvate carboxylase. *Biochem. J. 340* (Pt 1), 1–16.
3. Cronan, J. E., Jr. (2001) The biotinyl domain of *Escherichia coli* acetyl-CoA carboxylase. Evidence that the "thumb" structure is essential and that the domain functions as a dimer. *J. Biol. Chem. 276*, 37355–37364.
4. Janiyani, K., Bordelon, T., Waldrop, G. L., and Cronan, J. E., Jr. (2001) Function of *Escherichia coli* biotin carboxylase requires catalytic activity of both subunits of the homodimer. *J. Biol. Chem. 276*, 29864–29870.
5. Blanchard, C. Z., Chapman-Smith, A., Wallace, J. C., and Waldrop, G. L. (1999) The biotin domain peptide from the biotin carboxyl carrier protein of *Escherichia coli* acetyl-CoA carboxylase causes a marked increase in the catalytic efficiency of biotin carboxylase and carboxyltransferase relative to free biotin. *J. Biol. Chem. 274*, 31767–31769.
6. Blanchard, C. Z., Lee, Y. M., Frantom, P. A., and Waldrop, G. L. (1999) Mutations at four active site residues of biotin carboxylase abolish substrate-induced synergism by biotin. *Biochemistry 38*, 3393–3400.
7. Levert, K. L., Lloyd, R. B., and Waldrop, G. L. (2000) Do cysteine 230 and lysine 238 of biotin carboxylase play a role in the activation of biotin? *Biochemistry 39*, 4122–4128.
8. Waldrop, G. L., Rayment, I., and Holden, H. M. (1994) Three-dimensional structure of the biotin carboxylase subunit of acetyl-CoA carboxylase. *Biochemistry 33*, 10249–10256.
9. Athappilly, F. K., and Hendrickson, W. A. (1995) Structure of the biotinyl domain of acetyl-coenzyme A carboxylase determined by MAD phasing. *Structure 3*, 1407–1419.
10. Reddy, D. V., Shenoy, B. C., Carey, P. R., and Sonnichsen, F. D. (2000) High resolution solution structure of the 1.3S subunit of transcarboxylase from *Propionibacterium shermanii*. *Biochemistry 39*, 2509–2516.
11. Roberts, E. L., Shu, N., Howard, M. J., Broadhurst, R. W., Chapman-Smith, A., Wallace, J. C., Morris, T., Cronan, J. E., Jr., and Perham, R. N. (1999) Solution structures of apo and holo biotinyl domains from acetyl coenzyme A carboxylase of *Escherichia coli* determined by triple-resonance nuclear magnetic resonance spectroscopy. *Biochemistry 38*, 5045–5053.
12. Yao, X., Wei, D., Soden, C., Jr., Summers, M. F., and Beckett, D. (1997) Structure of the carboxy-terminal fragment of the apo-biotin carboxyl carrier subunit of *Escherichia coli* acetyl-CoA carboxylase. *Biochemistry 36*, 15089–15100.
13. Lane, M. D., and Lynen, F. (1963) The biochemical function of biotin, VI. Chemical structure of the carboxylated active site of propionyl carboxylase. *Proc. Natl. Acad. Sci. U. S. A. 49*, 379–385.
14. Blanchard, C. Z., and Waldrop, G. L. (1998) Overexpression and kinetic characterization of the carboxyltransferase component of acetyl-CoA carboxylase. *J. Biol. Chem. 273*, 19140–19145.
15. Levert, K. L., and Waldrop, G. L. (2002) A bisubstrate analog inhibitor of the carboxyltransferase component of acetyl-CoA carboxylase. *Biochem. Biophys. Res. Commun. 291*, 1213–1217.
16. Zhang, H., Tweel, B., and Tong, L. (2004) Molecular basis for the inhibition of the carboxyltransferase domain of acetyl-coenzyme-A carboxylase by haloxyfop and diclofop. *Proc. Natl. Acad. Sci. U. S. A. 101*, 5910–5915.

17. Diacovich, L., Peiru, S., Kurth, D., Rodriguez, E., Podesta, F., Khosla, C., and Gramajo, H. (2002) Kinetic and structural analysis of a new group of acyl-CoA carboxylases found in *Streptomyces coelicolor* A3(2). *J. Biol. Chem. 277*, 31228–31236.
18. Rodriguez, E., Banchio, C., Diacovich, L., Bibb, M. J., and Gramajo, H. (2001) Role of an essential acyl coenzyme A carboxylase in the primary and secondary metabolism of *Streptomyces coelicolor* A3(2). *Appl. Environ. Microbiol. 67*, 4166–4176.
19. Rodriguez, E., and Gramajo, H. (1999) Genetic and biochemical characterization of the alpha and beta components of a propionyl-CoA carboxylase complex of *Streptomyces coelicolor* A3(2). *Microbiology 145* (Pt 11), 3109–3119.
20. Pfeifer, B. A., Admiraal, S. J., Gramajo, H., Cane, D. E., and Khosla, C. (2001) Biosynthesis of complex polyketides in a metabolically engineered strain of *E. coli*. *Science 291*, 1790–1792.
21. Cane, D. E., Walsh, C. T., and Khosla, C. (1998) Harnessing the biosynthetic code: combinations, permutations, and mutations. *Science 282*, 63–68.
22. Khosla, C., and Keasling, J. D. (2003) Metabolic engineering for drug discovery and development. *Nat. Rev. Drug Discovery 2*, 1019–1025.
23. Lau, J., Fu, H., Cane, D. E., and Khosla, C. (1999) Dissecting the role of acyltransferase domains of modular polyketide synthases in the choice and stereochemical fate of extender units. *Biochemistry 38*, 1643–1651.
24. Liou, G. F., Lau, J., Cane, D. E., and Khosla, C. (2003) Quantitative analysis of loading and extender acyltransferases of modular polyketide synthases. *Biochemistry 42*, 200–207.
25. Watanabe, K., Khosla, C., Stroud, R. M., and Tsai, S. C. (2003) Crystal structure of an Acyl-ACP dehydrogenase from the FK520 polyketide biosynthetic pathway: insights into extender unit biosynthesis. *J. Mol. Biol. 334*, 435–444.
26. Diacovich, L., Mitchell, D. L., Pham, H., Gago, G., Melgar, M. M., Khosla, C., Gramajo, H., and Tsai, S. C. (2004) Crystal structure of the beta-subunit of acyl-CoA carboxylase: structure-based engineering of substrate specificity. *Biochemistry 43*, 14027–14036.
27. Otwinoswski, Z., and Minor, W. (1997) Processing of X-ray diffraction data collected in oscillation mode. *Methods Enzymol. 276*, 307–326.
28. Brunger, A. T., Adams, P. D., Clore, G. M., DeLano, W. L., Gros, P., Grosse-Kunstleve, R. W., Jiang, J. S., Kuszewski, J., Nilges, M., Pannu, N. S., Read, R. J., Rice, L. M., Simonson, T., and Warren, G. L. (1998) Crystallography & NMR system: A new software suite for macromolecular structure determination. *Acta Crystallogr. D Biol. Crystallogr. 54* (Pt 5), 905–921.
29. Munday, M. R. (2002) Regulation of mammalian acetyl-CoA carboxylase. *Biochem. Soc. Trans. 30*, 1059–1064.
30. Cronan, J. E., Jr., and Waldrop, G. L. (2002) Multi-subunit acetyl-CoA carboxylases. *Prog. Lipid Res. 41*, 407–435.
31. Lopaschuk, G. D., and Gamble, J. (1994) The 1993 Merck Frosst Award. Acetyl-CoA carboxylase: an important regulator of fatty acid oxidation in the heart. *Can. J. Physiol. Pharmacol. 72*, 1101–1109.
32. Tong, L., and Harwood, H. J., Jr. (2006) Acetyl-coenzyme A carboxylases: versatile targets for drug discovery. *J. Cell. Biochem. 99*, 1476–1488.
33. Gronwald, J. W. (1994) Herbicides inhibiting acetyl-CoA carboxylase. *Biochem. Soc. Trans. 22*, 616–621.
34. Ruderman, N. B., Park, H., Kaushik, V. K., Dean, D., Constant, S., Prentki, M., and Saha, A. K. (2003) AMPK as a metabolic switch in rat muscle, liver and adipose tissue after exercise. *Acta Physiol. Scand. 178*, 435–442.
35. Magnard, C., Bachelier, R., Vincent, A., Jaquinod, M., Kieffer, S., Lenoir, G. M., and Venezia, N. D. (2002) BRCA1 interacts with acetyl-CoA carboxylase through its tandem of BRCT domains. *Oncogene 21*, 6729–6739.
36. Kuhajda, F. P. (2000) Fatty-acid synthase and human cancer: new perspectives on its role in tumor biology. *Nutrition 16*, 202–208.
37. Zhang, H., Tweel, B., Li, J., and Tong, L. (2004) Crystal structure of the carboxyltransferase domain of acetyl-coenzyme A carboxylase in complex with CP-640186. *Structure* (*Cambridge*) *12*, 1683–1691.
38. Gago, G., Kurth, D., Diacovich, L., Tsai, S. C., and Gramajo, H. (2006) Biochemical and structural characterization of an essential acyl coenzyme A carboxylase from Mycobacterium tuberculosis. *J. Bacteriol. 188*, 477–486.
39. Lin, T. W., Melgar, M. M., Kurth, D., Swamidass, S. J., Purdon, J., Tseng, T., Gago, G., Baldi, P., Gramajo, H., and Tsai, S. C. (2006) Structure-based inhibitor design of AccD5, an essential acyl-CoA carboxylase carboxyltransferase domain of Mycobacterium tuberculosis. *Proc. Natl. Acad. Sci. U. S. A. 103*, 3072–3077.
40. Kurth, D. G., Gago, G. M., de la Iglesia, A., Bazet Lyonnet, B., Lin, T. W., Morbidoni, H. R., Tsai, S. C., Gramajo, H. (2009) Accase 6 is the essential acetyl-CoA carboxylase involved in fatty acid and mycolic acid biosynthesis in mycobacteria, *Microbiology* 155, 2664−2675.
41. Bhatnagar, R. S., Schall, O. F., Jackson-Machelski, E., Sikorski, J. A., Devadas, B., Gokel, G. W., and Gordon, J. I. (1997) Titration calorimetric analysis of AcylCoA recognition by myristoylCoA:protein N-myristoyltransferase. *Biochemistry 36*, 6700–6708.
42. Peterson, K. L., Peterson, K. M., and Srivastava, D. K. (1998) Thermodynamics of ligand binding and catalysis in human liver medium-chain acyl-CoA dehydrogenase: comparative studies involving normal and 3′-dephosphorylated C8-CoAs and wild-type and Asn191 → Ala (N191A) mutant enzymes. *Biochemistry 37*, 12659–12671.
43. Faergeman, N. J., Sigurskjold, B. W., Kragelund, B. B., Andersen, K. V., and Knudsen, J. (1996) Thermodynamics of ligand binding to acyl-coenzyme A binding protein studied by titration calorimetry. *Biochemistry 35*, 14118–14126.